

# Diffusion weighted imaging of prostate cancer xenografts: comparison of bayesian modeling and independent least squares fitting

Parisa Movahedi<sup>1</sup>, Hanne Hakkarainen<sup>2</sup>, Harri Merisaari<sup>1</sup>, Heidi Liljenbäck<sup>1</sup>, Helena Virtanen<sup>1</sup>, Hannu Juhani Aronen<sup>1</sup>, Heikki Minn<sup>1</sup>, Matti Poutanen<sup>1</sup>, Anne Roivainen<sup>1</sup>, Timo Liimatainen<sup>2</sup>, and Ivan Jambor<sup>1</sup>

<sup>1</sup>University of Turku, Turku, Finland, <sup>2</sup>A.I. Virtanen Institute for Molecular Sciences, Kuopio, Finland

## Synopsis

**Tumor growth in mice preclinical prostate cancer model (human prostate cancer cells, PC-3) was followed for 4 weeks by weekly DWI in control group (n=10) and treatment group (n=9) receiving Docetaxel. DWI data sets were acquired using 15 b-values in the range of 0-500s/mm<sup>2</sup> and 12 b-values the range of 0-2000 s/mm<sup>2</sup>. The DWI signal decays were fitted using monoexponential, biexponential, kurtosis and stretched exponential models/functions. Bayesian shrinkage prior method and independent least squares fitting have been applied and fitting quality evaluated by corrected Akaike Information Criteria. Bayesian modeling improved quality of DWI parametric maps derived using high b-value DWI data sets. Our result does not support the use of biexponential, kurtosis and stretched exponential models/functions for low b value DWI data sets of PC-3 mice preclinical prostate cancer model.**

## Purpose

To evaluate different mathematical functions/models for DWI of mice preclinical prostate cancer model (human prostate cancer cells, PC-3) using Bayesian shrinkage prior method and independent least squares fitting.

## Methods

One million PC-3 (Anticancer Inc., USA) human prostate cancer cells were inoculated subcutaneously in immunodeficient mice (n=11, HSD: Athymic Nude Foxn 1nu, Harlan Laboratories, Indianapolis, IN, USA). All animal handling was conducted in accordance with the local ethics committee for the use and care of laboratory animals and the institutional animal care policies, which fully meet the requirements as defined in the U.S. National Institutes of Health guidelines on animal experimentation. The mice were divided into 2 groups: 1. control group (n=10), 2. treatment group (n=9). The treatment group received Docetaxel (Docetaxel, Actavis, Espoo, Finland) given once a week for three weeks as i.p. injections. The dose was 15mg/kg. Tumor growth in both of the groups was followed by weekly MRI examinations performed using a 7T MR scanner (7T Pharmascan, Bruker GmbH, Ettlingen, Germany) and a 72 mm volume transmitter (Bruker GmbH) and 10 mm surface receiver coil (Bruker GmbH). Multislice T2-weighted anatomical images covering the whole tumor area were obtained (TR/TE 2500 ms/33 ms, field of view (FOV) = 30 × 30 mm<sup>2</sup>, matrix size 256 × 256, 15 slices) to localize a slice with maximum tumor diameter for DWI measurements. Diffusion weighted single shot spin-echo echo planar imaging was applied with the parameters: TR/TE 3750/25.3 (low b-value set) 3000/30 ms (high b-

value set), FOV  $3 \times 1.5$  cm<sup>2</sup>, matrix  $128 \times 64$ , slice thickness 1 mm, three orthogonal diffusion directions, and two different sets of b-values: low b-value set (15 b-values in total): 0, 2, 4, 6, 9, 12, 14, 18, 23, 25, 28, 50, 100, 300, 500 s/mm<sup>2</sup>, and high b-value set (12 b-values in total): 0, 100, 300, 500, 700, 900, 1100, 1300, 1500, 1700, 1900, 2000 s/mm<sup>2</sup>. For further analysis, the mean value of the signal from three directions was calculated. The following four mathematical functions/models were applied to the DWI signal obtained using low and high b-values:

1. Mono-exponential model (1):

$$S(b) = S_0 e^{-bADC_m} \quad S(b) = S_0 e^{-bADC_m}$$

Eq. 1

2. Stretched exponential model (2):

$$S(b) = S_0 e^{-bADC_\alpha} \quad S(b) = S_0 e^{-bADC_\alpha}$$

Eq. 2

3. Kurtosis model (3):

$$S(b) = S_0 (e^{-bADC_k + 1/6 b^2 ADC_k^2 K}) \quad S(b) = S_0 (e^{-bADC_k + 1/6 b^2 ADC_k^2 K})$$

Eq. 3

4a. Bi-exponential model for low b-values (4):

$$S(b) = S_0 (f e^{-bD_p} + (1-f) e^{-bD_f}) \quad S(b) = S_0 (f e^{-bD_p} + (1-f) e^{-bD_f})$$

Eq. 4

4b. Bi-exponential model for high b-values (5):

$$S(b) = S_0 (f e^{-bD_f} + (1-f) e^{-bD_s}) \quad S(b) = S_0 (f e^{-bD_f} + (1-f) e^{-bD_s})$$

Eq. 5

The DWI signal decay of each individual voxel has been fitted using four mathematical models, as described above, to generate parametric maps of the parameters. The fitting procedure has been performed using the Levenberg–Marquardt algorithm in Python programming language and following multiple initialization values to prevent local minima in the fitting procedure. Furthermore, all of the parameters except of the Mono-exponential model's parameter ( $ADC_m$ ) have been fitted by a Bayesian shrinkage method (6). The Bayesian shrinkage prior (BSP) model takes the estimated parameters from least squares fit as a prior distribution of the region of interest, jointly estimating the voxel-wise parameters based on the ROI distribution. The Markove chain algorithm utilizing Gibbs sampling with Metropolis-Hastings updates for each voxel parameters has been applied to each ROI to robustly and quickly converge to the stationary distribution of each parameter. The tumor area was manually delineated on T2-weighted anatomical images and the regions of interest (ROIs) were transferor to the corresponding parametric images. Corrected Akaike information criteria difference (AICc) (7) was used to evaluate fitting quality.

## Results

The use of Bayesian shrinkage method resulted in reduced parameter variation (Figure 1) and smoother parametric maps (Figure 2) which could be attributed to reduced estimation uncertainty of each model. Bayesian shrinkage method resulted in approximately 20% and 40% increase in root measure error of the least square fitting procedure in high and low b-value data sets, respectively (Figure 3). In majority of voxels (above 50%) stretched exponential, kurtosis and bi-exponential models fitted DWI data obtained using high b-values better than the mono-exponential model based on AICc (Figure 4). The kurtosis model was preferred over the stretched exponential model in average in approximately ~70% of voxels. In contrast, stretched exponential, kurtosis and bi-exponential models were not preferred over the monoexponential model in DWI data obtained using low b-values (Figure 5).

## Conclusion

Bayesian modeling improved quality of DWI parametric maps derived using high b-value DWI data sets. Our result does not support the use of biexponential, kurtosis and stretched exponential models/functions for low b value DWI data sets of PC-3 mice preclinical prostate cancer model.

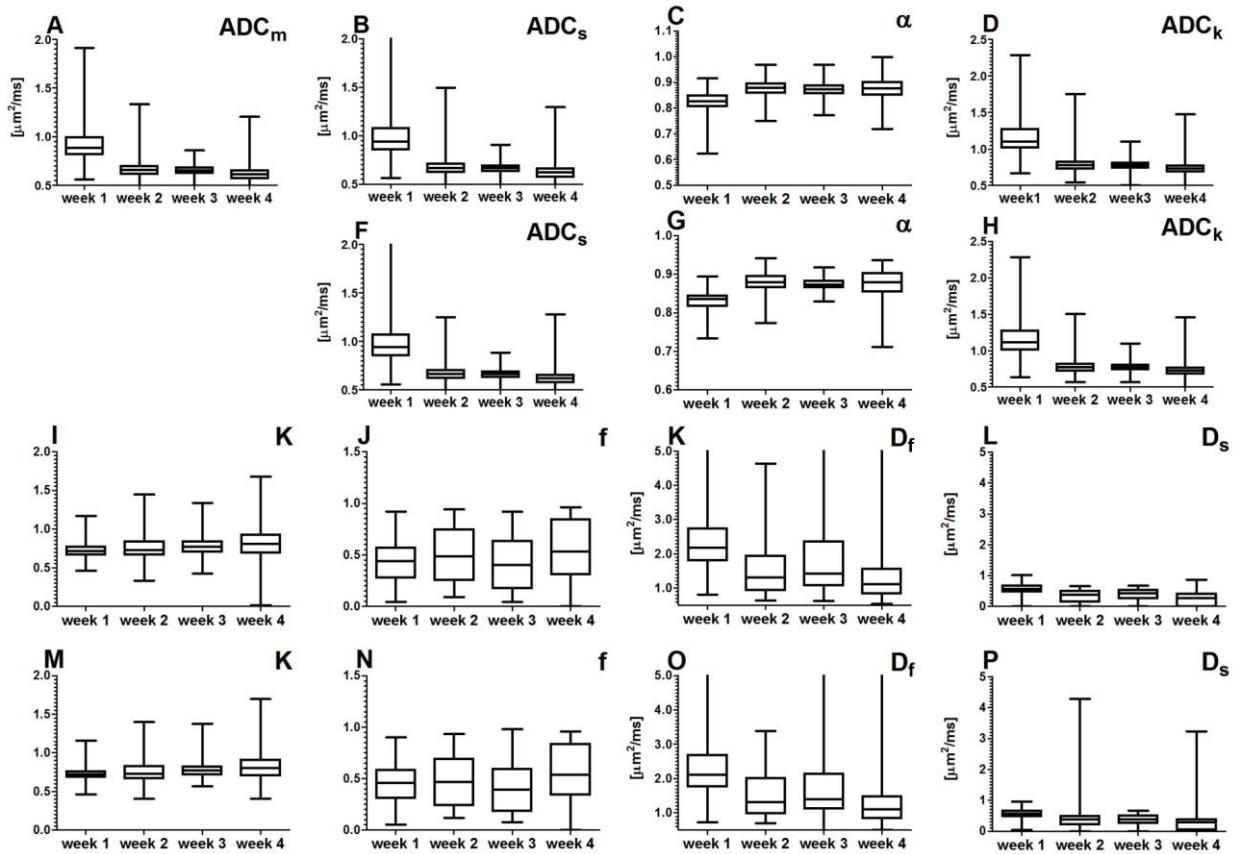
## Acknowledgements

No acknowledgement found.

## References

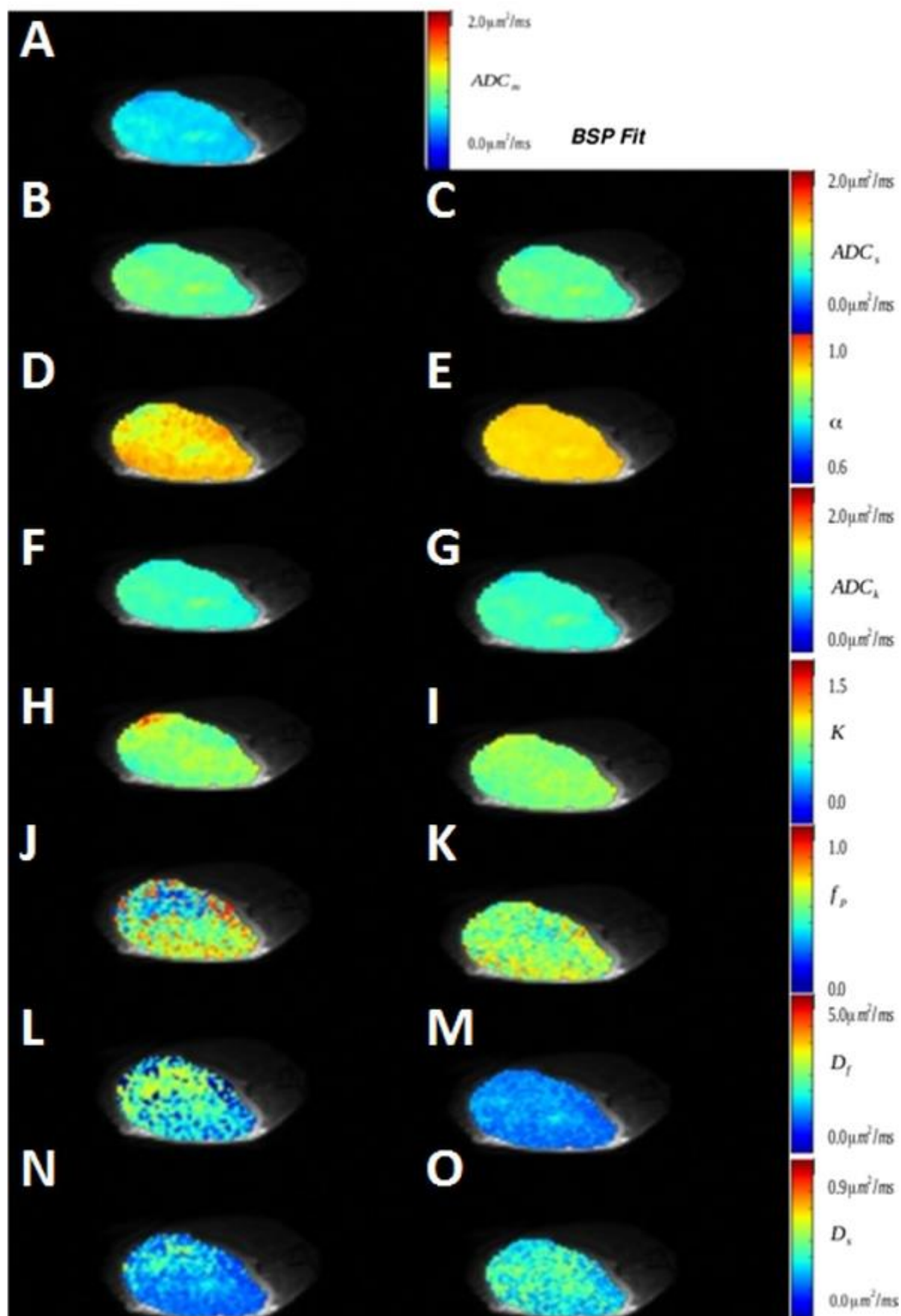
1. Stejskal EO. Use of spin echoes in a pulsed magnetic-field gradient to study restricted diffusion and flow. *J Chem Phys* 1965;43:3597–3603
2. Kopf M, Corinth C, Haferkamp O, Nonnenmacher TF. Anomalous diffusion of water in biological tissues. *Biophys J* 1996; 70:2950-2958.
3. Jensen JH, Helpert JA. MRI quantification of non-Gaussian water diffusion by kurtosis analysis. *NMR Biomed* 2010; 23:698-710.
4. Le Bihan D, Breton E, Lallemand D, Aubin ML, Vignaud J, Laval-Jeantet M. Separation of diffusion and perfusion in intravoxel incoherent motion MR imaging. *Radiology* 1988; 168:497-505.
5. Mulkern RV, Gudbjartsson H, Westin CF, et al. Multi-component apparent diffusion coefficients in human brain. *NMR Biomed* 1999; 12:51-62.
6. Orton MR, Collins DJ, Koh DM, Leach MO. Improved intravoxel incoherent motion analysis of diffusion weighted imaging by data driven Bayesian modeling. *Magn Reson Med* 2014; 71:411-420.
7. Akaike H. Information theory as an extension of the maximum likelihood principle. In: Petrov BN, Csaki F, editors. *Second International Symposium on Information Theory*. Budapest: Akademiai Kiado; 1973. p 267–281.

## Figures



Box plots of voxel values derived using independent least squares fitting (A, B, C, D, I, J, K, L) and bayesian shrinkage method (F, G, H, M, N, O, P) for high b values data sets of control group.  $\text{ADC}_m$  parameter (A) was estimated only using independent least squares fitting. The box extends from the 25th to 75th percentiles while the error bars extend from minimal to maximal values.

LSQ Fit





Parametric maps using independent least squares fitting, LSG fit, (A, B, D, F, H, J, L, N) and Bayesian shrinkage method, BSP Fit, (C, E, G, I, K, M, O) for high b value data sets of control group mice in week 3. ADCm parameter (A) was estimated only using independent least squares fitting.

	Biexponential	Kurtosis	Stretched
Control Group (high b-values)	20%	25%	19%
Treatment Group (high b-values)	21%	23%	18%
Control Group (low b-values)	23%	49%	33%
Treatment Group (low b-values)	43%	32%	36%

Median percentage value of root mean square error increase of the bayesian shrinkage method over independent least squares fitting.

<b>Control group (High b-values)</b>	week1	week2	week3	week4
Stretched vs. Mono	100%	99%	100%	99%
Kurtosis vs. Mono	100%	100%	99%	99%
Biexp vs. Mono	99%	99%	100%	97%
Kurtosis vs. Stretched	70%	73%	71%	76%
Biexp vs. Stretched	80%	76%	64%	59%
Biexp vs. Kurtosis	57%	37%	26%	13%
Stretched (Bayesian) vs. Mono	97%	91%	94%	89%
Kurtosis (Bayesian) vs. Mono	98%	97%	97%	95%
Biexp (Bayesian) vs. Mono	100%	99%	100%	99%
Kurtosis (Bayesian) vs. Stretched (Bayesian)	63%	67%	66%	67%
Biexp (Bayesian) vs. Stretched (Bayesian)	78%	72%	62%	62%
Biexp (Bayesian) vs. Kurtosis (Bayesian)	67%	50%	39%	37%
<b>Treatment group (High b-values)</b>	week1	week2	week3	week4
Stretched vs. Mono	97%	99%	99%	100%
Kurtosis vs. Mono	98%	99%	99%	99%
Biexp vs. Mono	95%	99%	98%	98%
Kurtosis vs. Stretched	89%	78%	75%	71%
Biexp vs. Stretched	86%	40%	83%	72%
Biexp vs. Kurtosis	28%	16%	49%	56%
Stretched (Bayesian) vs. Mono	48%	37%	6%	8%
Kurtosis (Bayesian) vs. Mono	24%	26%	4%	4%
Biexp (Bayesian) vs. Mono	99%	100%	100%	98%
Kurtosis (Bayesian) vs. Stretched (Bayesian)	34%	55%	41%	70%
Biexp (Bayesian) vs. Stretched (Bayesian)	80%	51%	77%	67%
Biexp (Bayesian) vs. Kurtosis (Bayesian)	39%	33%	46%	60%

High b-value DWI data sets: Selection of preferred model in different groups, each comparing two models. Percentage of ROIs described better by the first model of the comparison is shown in the table.

<b>Control group (Low b-values)</b>	week1	week2	week3	week4
Stretched vs. Mono	79%	70%	71%	81%
Kurtosis vs. Mono	77%	61%	64%	57%
Biexp vs. Mono	68%	41%	46%	77%
Kurtosis vs. Stretched	19%	23%	29%	12%
Biexp vs. Stretched	29%	11%	10%	40%
Biexp vs. Kurtosis	51%	30%	29%	71%
Stretched (Bayesian) vs. Mono	47%	18%	21%	25%
Kurtosis (Bayesian) vs. Mono	8%	16%	13%	9%
Biexp (Bayesian) vs. Mono	43%	17%	12%	42%
Kurtosis (Bayesian) vs. Stretched (Bayesian)	21%	26%	34%	22%
Biexp (Bayesian) vs. Stretched (Bayesian)	37%	41%	21%	50%
Biexp (Bayesian) vs. Kurtosis (Bayesian)	62%	49%	37%	62%
<b>Treatment group (Low b-values)</b>	week1	week2	week3	week4
Stretched vs. Mono	78%	70%	46%	39%
Kurtosis vs. Mono	79%	66%	55%	22%
Biexp vs. Mono	64%	63%	21%	16%
Kurtosis vs. Stretched	18%	23%	66%	17%
Biexp vs. Stretched	5%	31%	7%	1%
Biexp vs. Kurtosis	33%	57%	10%	9%
Stretched (Bayesian) vs. Mono	49%	37%	6%	8%
Kurtosis (Bayesian) vs. Mono	24%	25%	4%	4%
Biexp (Bayesian) vs. Mono	26%	20%	6%	4%
Kurtosis (Bayesian) vs. Stretched (Bayesian)	34%	55%	41%	70%
Biexp (Bayesian) vs. Stretched (Bayesian)	17%	23%	26%	13%
Biexp (Bayesian) vs. Kurtosis (Bayesian)	44%	26%	27%	12%

Low b-value DWI data sets: Selection of preferred model in different groups, each comparing two models. Percentage of ROIs described better by the first model of the comparison is shown in the table.